Lanthanides or Dust in Kilonovae

Lessons Learned from GW170817

Gall, Christa; Hjorth, Jens; Rosswog, Stephan; Tanvir, Nial R.; Levan, Andrew J.

Published in:
Astrophysics Journal Letters

DOI:
10.3847/2041-8213/aa93f9

Publication date:
2017

Document version
Publisher's PDF, also known as Version of record

The Astrophysical Journal Letters, 849:L19 (5pp), 2017 November 10 https://doi.org/10.3847/2041-8213/aa93f9

Lanthanides or Dust in Kilonovae: Lessons Learned from GW170817

Christa Gall[1], Jens Hjorth[1], Stephan Rosswog[2], Nial R. Tanvir[3], and Andrew J. Levan[4]
[1] Dark Cosmology Centre, Niels Bohr Institute, University of Copenhagen, Juliane Maries Vej 30, DK-2100 Copenhagen Ø, Denmark
[2] The Oskar Klein Centre, Department of Astronomy, AlbaNova, Stockholm University, SE-106 91 Stockholm, Sweden
[3] Department of Physics and Astronomy, University of Leicester, Leicester LE1 7RH, UK
[4] Department of Physics, University of Warwick, Coventry CV4 7AL, UK
Received 2017 October 9; revised 2017 October 13; accepted 2017 October 14; published 2017 November 2

Abstract

The unprecedented optical and near-infrared lightcurves of the first electromagnetic counterpart to a gravitational-wave source, GW170817, a binary neutron star merger, exhibited a strong evolution from blue to near-infrared (a so-called "kilonova" or "macronova"). The emerging near-infrared component is widely attributed to the formation of *r*-process elements that provide the opacity to shift the blue light into the near-infrared. An alternative scenario is that the light from the blue component gets extinguished by dust formed by the kilonova and subsequently is re-emitted at near-infrared wavelengths. We test here this hypothesis using the lightcurves of AT 2017gfo, the kilonova accompanying GW170817. We find that of the order of $10^{-5}\,M_{\odot}$ of carbon is required to reproduce the optical/near-infrared lightcurves as the kilonova fades. This putative dust cools from ∼2000 K at ∼4 days after the event to ∼1500 K over the course of the following week, thus requiring dust with a high condensation temperature, such as carbon. We contrast this with the nucleosynthetic yields predicted by a range of kilonova wind models. These suggest that at most $10^{-9}\,M_{\odot}$ of carbon is formed. Moreover, the decay in the inferred dust temperature is slower than that expected in kilonova models. We therefore conclude that in current models of the blue component of the kilonova, the near-infrared component in the kilonova accompanying GW170817 is unlikely to be due to dust.

Key words: binaries: general – dust, extinction – gravitational waves – infrared: stars – stars: neutron

1. Introduction

The detection of electromagnetic radiation from a gravitational-wave event has heralded in a new era in multi-messenger astronomy (Abbott et al. 2017a). LIGO detected gravitational waves (GW170817) from a binary neutron star merger (Abbott et al. 2017b) that were localized by LIGO and Virgo to a 28 deg^2 region. Coincident in time, a short gamma-ray burst (GRB 170817A) was detected by the *Fermi* Gamma-ray Telescope (Goldstein et al. 2017) and *INTEGRAL* (Savchenko et al. 2017). The source (initially named SSS17a or DLT17ck; see Abbott et al. 2017a) was subsequently accurately localized at optical (Coulter et al. 2017) and near-infrared (Tanvir et al. 2017) wavelengths, 10″ from the nucleus of the S0/E galaxy NGC 4993 (Levan et al. 2017) at $z = 0.0098$, corresponding to an "electromagnetic luminosity distance" of 41.0 ± 3.1 Mpc (Hjorth et al. 2017) or a "gravitational-wave luminosity distance" of $43.8^{+2.9}_{-6.9}$ Mpc (Abbott et al. 2017c).

The electromagnetic counterpart, henceforth named AT 2017gfo, evolved from blue to red (Pian et al. 2017; Tanvir et al. 2017), broadly interpreted as being due to a kilonova (Metzger et al. 2010), consisting of an outflow ("wind") of material with a high electron fraction,[5] Y_e, (Metzger & Fernández 2014) as well as a low Y_e, dynamic ejecta "third peak" *r*-process kilonova (Barnes & Kasen 2013; Tanvir et al. 2013; Rosswog et al. 2017). However, the existence of very heavy elements, e.g., lanthanides, is only inferred indirectly as being required to produce the opacity needed to shift the UV/optical emission into the near-infrared (Tanvir et al. 2017).

Given that this is an unprecedented event, it is worthwhile exploring other suggested scenarios. Indeed, inspired by the first detection of a likely kilonova accompanying GRB 130603B by Tanvir et al. (2013; see also Berger et al. 2013), Takami et al. (2014) predicted that the evolution of a high-density wind would evolve from blue to red due to dust formed in the kilonova. The hot, newly formed dust would lead to obscuration in the blue and re-emission in the near-infrared, thus mimicking the effect of high-opacity lanthanides.

Here, we explore this scenario in view of the spectacular multi-wavelength optical and near-infrared lightcurves (Tanvir et al. 2017) and spectra (Pian et al. 2017; Tanvir et al. 2017) that were obtained for AT 2017gfo. We present dust model fits in Section 2 and discuss carbon masses predicted in kilonova models in Section 3. We compare those to the required dust mass in carbon and discuss our results in Section 4.

2. Fitting Dust Models to Kilonova Data

We use the *rYJKs*-band photometric data of AT 2017gfo obtained by Tanvir et al. (2017) to constrain possible dust emission from the kilonova. Lightcurve fits were presented by Gompertz et al. (2017). These are entirely phenomenological representations of the data points and are based on four-parameter parameterizations, involving a normalization, a rise time constant, a peak time, and a decay time constant (Bazin et al. 2011). As such, they do not assume anything about the spectral energy distribution and they are not physically motivated by kilonova models. The lightcurve fits are constrained by suitable extinction-corrected data points, starting half a day after the event in the near-infrared bands and a day later in the *r* band. The last data points were obtained at about 9.5–11.5 days in *rYJ* and at 25 day in *Ks* (Tanvir et al. 2017). We use here the lightcurve fits and note that

[5] It is worth stressing that what is called "high Y_e" means $Y_e > 0.25$, so that no lanthanides are produced. In other contexts, such values are still considered as low Y_e.

Table 1
Yields

Conditions	X_C	X_O	X_{Mg}	X_{Si}	X_{Fe}	X_{A70}	X_{A130}	Comments
hydro sim.: (1.3 + 1.3) $M_\odot$	1.6×10^{-8}	1.9×10^{-6}	1.1×10^{-5}	4.7×10^{-7}	3.8×10^{-6}	9.92×10^{-2}	8.39×10^{-2}	dynamic ejecta[a]
hydro sim.: (1.4 + 1.8) $M_\odot$	4.6×10^{-10}	1.7×10^{-5}	1.9×10^{-5}	3.0×10^{-5}	4.6×10^{-6}	9.90×10^{-2}	8.39×10^{-2}	dynamic ejecta[b]
wind $Y_e = 0.28$, $v = 0.1c$	4.6×10^{-13}	4.2×10^{-7}	3.9×10^{-9}	7.7×10^{-10}	9.2×10^{-7}	9.99×10^{-2}	1.5×10^{-3}	...
wind: $Y_e = 0.35$, $v = 0.1c$	2.0×10^{-20}	3.9×10^{-19}	3.9×10^{-9}	4.6×10^{-19}	9.2×10^{-4}	9.61×10^{-2}	4.7×10^{-5}	higher Y_e
wind: $Y_e = 0.45$, $v = 0.05c$	3.1×10^{-7}	5.2×10^{-10}	1.1×10^{-9}	8.4×10^{-9}	6.1×10^{-4}	1.87×10^{-2}	0.0	very high Y_e[c]

Notes.
[a] Run "N2" from Rosswog et al. (2017).
[b] Run "N5" from Rosswog et al. (2017).
[c] Not expected to be a likely case.

extrapolated lightcurves may be uncertain as they rely on the validity of the adopted parameterization.

Assuming the near-infrared emission is due to dust, we fit a modified blackbody function (Hildebrand 1993) to the lightcurves:

$$F_\nu(\nu) = \frac{M_d}{D_L^2}\,\kappa_{abs}(\nu, a)\,B_\nu(\nu, T_d), \quad (1)$$

where M_d is the mass of dust, D_L is the luminosity distance to GW170817 (Hjorth et al. 2017), and $B_\nu(\nu, T_d)$ is the Planck function at temperature T_d for the dust. Here, $\kappa_{abs}(\nu, a)$ is the dust mass absorption coefficient (in units of [$cm^2\,g^{-1}$]) for an assumed dust composition and grain size a, e.g., amorphous carbon (Rouleau & Martin 1991) or silicates (Li & Draine 2001). Equation (1) describes an ensemble of dust grains, each emitting a blackbody spectrum, and takes the $\kappa_{abs}(\nu, a)$ dependence on wavelength and grain size of each individual dust species into account.

As visualized in Figure 1, $\kappa_{abs}(\nu, a)$ behaves as a λ^{-x} power law in the wavelength range 0.9–2.5 μm. Therefore, we parameterize the absorption coefficient as

$$\kappa_{abs}(\lambda) = A_d\left(\frac{\lambda}{1\ \mu m}\right)^{-x}, \quad (2)$$

where A_d represents the value of $\kappa_{abs}(\lambda = 1\ \mu m)$ and x is the power-law slope.

Takami et al. (2014) argued that the near-infrared detection of a kilonova in GRB 130313B suggests a high dust temperature (~2000 K), which would single out carbon as the only viable dust species, due to its high condensation temperature. To explore this suggestion, we assume a $\kappa_{abs}(\lambda)$ model corresponding to carbonaceous dust. A value of $x = 1.2$ (similar to Zubko et al. 1996) was assumed by Takami et al. (2014). To cover the range depicted in Figure 1, we vary A_d between 9×10^3 and 1.1×10^4 $cm^2\,g^{-1}$ and adopt power-law exponents of either $x = 1.2$ or 1.5. We fit for T_d and M_d.

Figure 2 shows the modified blackbody fits to the lightcurves at arbitrary times. Initially, the spectral energy distribution of AT 2017gfo is blue, but at later times, the data points are well represented by the modified blackbody fits. The differences in the fits are small when using either $x = 1.2$ or 1.5, although the $x = 1.5$ models provide slightly better fits.

Figure 3 shows that the dust temperature is above ~2000 K when dust formation sets in at around 4 days (in this scenario). This is consistent with the estimates of Takami et al. (2014) and underlines why carbon, with its high condensation temperature, is the best candidate for kilonova dust. Over the course of the

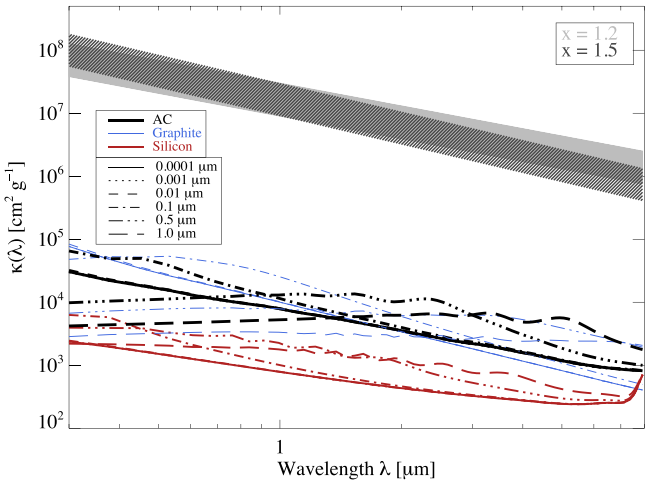

Figure 1. Dust mass absorption coefficient $\kappa_{abs}(\lambda)$ for amorphous carbon (black), graphite (blue), and silicon (red) dust for grain sizes varying between 0.0001 and 1.0 μm. The gray shaded regions represent the $\kappa_{abs}(\lambda)$ required to reproduce the spectra energy distribution for a fixed amount of carbon of $10^{-9}\,M_\odot$.

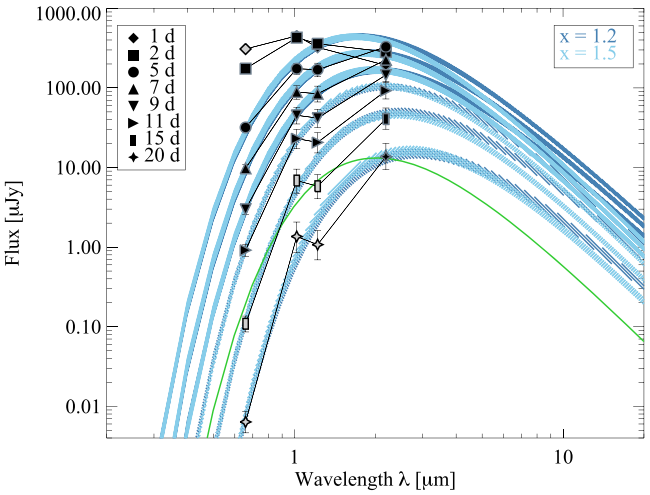

Figure 2. Modified blackbody (Equation (1)) fits to the spectral energy distribution of AT 2017gfo at a range of arbitrary epochs. Points outside ranges sampled by data points (i.e., extrapolated lightcurves) are indicated as open symbols with error bars reflecting the formal uncertainties in the extrapolations. The fitted carbon models (Equation (2)) are shown as shaded blue curves, indicating the uncertainties in the fits. The green solid curve represents a modified blackbody curve consistent with the K-band value at 20 days for average carbon dust parameters ($A_d = 1.0 \times 10^4$ $cm^2\,g^{-1}$, $x = 1.5$), $T_d = 1600$ K, and $M_d \sim 5.7 \times 10^{-7}\,M_\odot$.

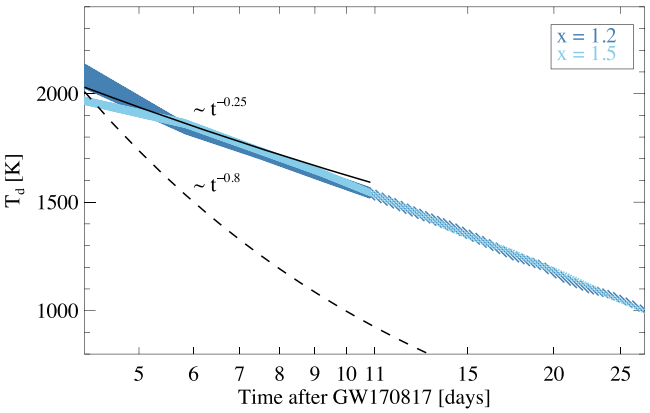

Figure 3. Evolution of the dust temperature as inferred from the modified blackbody fits. The shaded areas reflect the 3σ range around the average dust temperature of models with $A_{\rm d} = 0.9$, 1.0, 1.1×10^4 cm^2 g^{-1}. The fact that the dark blue ($x = 1.2$) and light blue ($x = 1.5$) almost coincide reflect the insensitivity of the results to the adopted value of x. Dust temperatures beyond 11 days are shown with a lighter shade to reflect that they rely on extrapolated lightcurve fits. During the first week, the dust temperature roughly evolves as $\propto t^{-0.25}$ (black curve), after which it steepens. The dashed black curve represents the expected kilonova temperature evolution (e.g., Grossman et al. 2014).

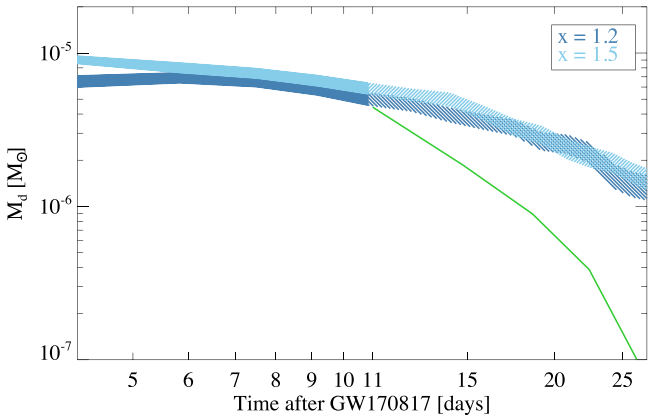

Figure 4. Evolution of the dust mass, corresponding to the dust temperature evolution in Figure 3. Dust masses beyond 11 days are shown with a lighter shade to reflect that they rely on extrapolated lightcurve fits. The green solid curve represents the lower limit on $M_{\rm d}$ derived from a modified blackbody to the single K-band values between 11 and 30 days for an average carbon dust composition ($A_{\rm d} = 1.0 \times 10^4$ cm^2 g^{-1}, $x = 1.5$) and $T_{\rm d} = 1600$ K.

following week, the dust temperature drops to about $\sim$1500 K. The temperature evolution is insensitive to the choice of x. Beyond this time, the lightcurve fits are constrained by the *Ks*-band data only and so the fitted dust models rely on extrapolations of the lightcurve representations. The dust temperature drops below $\sim$1000 K at about 26 days according to these fits.

The inferred dust temperature roughly decays as $T_{\rm d} \propto t^{-s}$, with $s = 0.25$, quite different from that expected in kilonova models (Grossman et al. 2014), namely, $s = (\alpha + 2)/4 \approx 0.8$ for a heating rate $\propto t^{-\alpha}$, with $\alpha = 1.2$–1.3. In fact, $s = 0.25$ would correspond to an unrealistic, linearly increasing heating rate, $\alpha = -1.0$.

Figure 4 shows the inferred dust mass as a function of time. The dust mass is consistent with being constant, at about (6–7) $\times 10^{-6}$ $M_\odot$ up to 11 days, i.e., during the time span where the lightcurve fits are strongly constrained by data. Beyond this time, the inferred dust mass appears to drop. This finding relies to some extent on the validity of the lightcurve extrapolations in the *rYJ* bands. Using only the *Ks*-band data we can derive a lower limit on carbon dust for epochs beyond 11 days for a given temperature. Adopting $T_{\rm d} = 1600$ K, which is the derived temperature at 11 days, as an upper limit to the temperature for any subsequent epochs, we obtain a lower limit to the needed carbon dust mass of $\sim 2 \times 10^{-6}\,M_\odot$ at 15 days dropping to $\sim 2 \times 10^{-7}\,M_\odot$ at 25 days (a modified blackbody fit at 20 days is shown in Figure 2 as a green curve).

Spitzer Space Telescope observed AT 2017gfo on 2017 September 29 (Lau et al. 2017), about 43 days after the gravitational-wave event. The extrapolated *Ks*-band lightcurve suggests $K_{\rm AB} = 26.5 \pm 0.7$ and the dust models with a $T_{\rm d} = 740 \pm 200$ K predict $K_{\rm AB} - m_{3.6\mu{\rm m}} = 0.97 \pm 1.5$, i.e., $m_{3.6\mu{\rm m}} = 25.5 \pm 1.7$ and $K_{\rm AB} - m_{4.5\mu{\rm m}} = 1.06 \pm 1.3$, i.e., $m_{4.5\mu{\rm m}} = 25.45 \pm 1.5$.

3. Carbon Production in Kilonovae

Nucleosynthetic models based on neutrino-driven winds, consistent with the Takami et al. (2014) scenario of a high Y_e wind as the origin of the blue kilonova, suggest a total ejected mass of the order of $10^{-2}\,M_\odot$ and a very small abundance of carbon (Dessart et al. 2009; Perego et al. 2014; Martin et al. 2015).

Another ejecta source that could produce more material is the unbinding of the accretion torus (e.g., Fernández & Metzger 2013; Ciolfi & Siegel 2015; Just et al. 2015; Martin et al. 2015; Siegel & Metzger 2017), which could provide $\sim$40% of the original torus mass. Depending on the mass ratio of the neutron stars, torus masses can easily reach $\sim 0.2\,M_\odot$ (Giacomazzo et al. 2013), so that an order of magnitude more mass can become unbound. This material may have similar properties, i.e., a larger Y_e and hence lower opacity.

We explore a broad range of wind ejecta models. They comprise different physical origins such as neutrino absorption or the unbinding of the accretion torus formed during the merger. The winds are set up as described in detail in Rosswog et al. (2017, their Section 2.2) and are parameterized by their initial entropy, their electron fraction Y_e, and their expansion velocity $v_{\rm ej}$. This parameter space has been explored with over 190 models where Y_e was varied between 0.05 and 0.45, and $v_{\rm ej}$ from 0.05 to 0.4c. To keep the parameter space under control the initial entropy was fixed to 15 k_B per baryon since detailed wind models (Perego et al. 2014) find a narrow distribution around this value. We use the WinNet nuclear reaction network (Winteler 2012); see Rosswog et al. (2017) for a more complete list of the ingredients. For electron fractions $Y_e \lesssim 0.3$, we find at maximum a carbon mass fraction of 10^{-8} (see Table 1), but in most cases values that are orders of magnitude lower. In one case ($Y_e = 0.45$, $v_{\rm ej} = 0.05$), we find $X_c = 3 \times 10^{-7}$, but such Y_e-values are not representative for the overall merger ejecta. Given an ejecta mass of a few 0.01 $M_\odot$, we consider a carbon mass of $10^{-9}\,M_\odot$ as a robust upper limit.

4. Discussion

We inspected a series of wind models and found a maximum mass fraction of $10^{-7}\,M_\odot$, suggesting a very small production of carbon of $10^{-9}\,M_\odot$ in such winds. In contrast, our dust models require of the order of $10^{-5}\,M_\odot$ of carbon dust to be consistent with the lightcurves of AT 2017gfo.

This discrepancy of four orders of magnitude is unlikely to be due to systematic errors in our approach, despite possible caveats:

1. We fit dust models to parameterized lightcurves (Gompertz et al. 2017). While the fits to the *rYJKs* bands are good representations of the data, there may be variations in the dust mass and dust temperature results when using the real data. However, we verified that the differences between the lightcurve fits and the real data fits are small. As already discussed, any results based on extrapolated lightcurves are more uncertain, but our main conclusions do not rely on fits outside the range of well-sampled lightcurves (1–11 days past the gravitational-wave event).
2. We have assumed that the dust is homogeneously distributed. Clumping may impact the resulting dust mass. However, a clumpy structure typically requires even higher dust masses (see, e.g., Gall et al. 2011 for supernova dust models).

One could imagine that other elements might contribute to the total dust mass budget. As noted by Takami et al. (2014), the main challenge with this scenario is that the high dust temperature required to fit the data practically rules out all other known dust species. While a blue kilonova is not expected to produce lanthanides, it does produce *r*-process elements. However, as discussed by Takami et al. (2014), these are unlikely to condense, despite their fairly high condensation temperatures, because of their low number densities.

Hypothetically, we have tested what would be the properties of $\kappa_{\rm abs}(\lambda)$ (for $x = 1.2$ or 1.5) in order to accommodate both an upper limit on the dust mass of $10^{-9}\,M_{\odot}$ and reproduce the observed spectral energy distribution. The result is shown as gray bands in Figure 1. Such $\kappa_{\rm abs}(\lambda)$ leads to modified blackbody fits and evolution of dust temperature and mass similar to those shown in Figures 2–4. However, they neither correspond to carbonaceous dust nor any other known dust species.

Moreover, an increased $\kappa_{\rm abs}(\lambda)$ would not explain the slow decline of the dust temperature (Figure 3), apparently requiring an unrealistic increasing rate of heating with time. This result is largely independent of the assumed properties and appears to rule out any type of dust.

The spectra of AT 2017gfo indicate significant absorption at near-infrared wavelengths (Pian et al. 2017; Tanvir et al. 2017), consistent with an interpretation in which *r*-process elements have formed. However, it is not proven that the absorption features are due to lanthanides that are required to shift blue emission into the near-infrared. Therefore, the absorption features do not by themselves rule out a hot dust emission origin of the near-infrared kilonova.

The larger Y_e material in both the neutrino-driven winds and the unbound torus will be concentrated toward the rotation axis of the binary (see, e.g., Figure 2 in Siegel & Metzger 2017), while the very heavy *r*-process material is more like a fat torus expanding in the orbital plane. Geometrically, we would therefore expect light elements to be unobscured when seen along the rotation axis, but potentially obscured when seen "edge-on." If they also form from the torus (which takes time to unbind; $\sim$1 s) such material could well be behind the earlier ejected heavy *r*-process, leading to absorption features in the hot dust emission component. Consequently, the significant absorption in the spectra of AT 2017gfo suggests that the inferred dust mass from the lightcurves represents a lower limit to the required dust mass.

We conclude that the simplest models with carbon dust forming out of the Y_e-rich ejecta is unlikely to produce the near-infrared emission. One would need a dust species with a high condensation temperature and a very high opacity (see Figure 1) or very large amounts of carbon to be produced to make the hot-dust emission model for the infrared component of kilonovae viable. For the time being, models in which high-opacity elements, such as lanthanides, are responsible for the near-infrared flux are favored (Tanvir et al. 2017).

C.G. acknowledges support from the Carlsberg Foundation. J.H. is supported by a VILLUM FONDEN Investigator grant (project number 16599). S.R. has been supported by the Swedish Research Council (VR) under grant number 2016-03657_3, by the Swedish National Space Board under grant number Dnr. 107/16, and by the research environment grant "Gravitational Radiation and Electromagnetic Astrophysical Transients (GREAT)" funded by the Swedish Research council (VR) under Dnr. 2016-06012. A.J.L. is supported by STFC and the ERC (grant #725246).

ORCID iDs

Christa Gall https://orcid.org/0000-0002-8526-3963
Jens Hjorth https://orcid.org/0000-0002-4571-2306
Nial R. Tanvir https://orcid.org/0000-0003-3274-6336

References

Abbott, B. P., Abbott, R., Abbott, T. D., et al. 2017a, ApJL, https://doi.org/10.3847/2041-8213/aa920c
Abbott, B. P., Abbott, R., Abbott, T. D., et al. 2017b, PhRvL, https://doi.org/10.1103/PhysRevLett.119.161101
Abbott, B. P., Abbott, R., Adhikari, R. X., et al. 2017c, Natur, https://doi.org/10.1038/nature24471
Barnes, J., & Kasen, D. 2013, ApJ, 775, 18
Bazin, G., Ruhlmann-Kleider, V., Palanque-Delabrouille, N., et al. 2011, A&A, 534, A43
Berger, E., Fong, W., & Chornock, R. 2013, ApJL, 774, L23
Ciolfi, R., & Siegel, D. M. 2015, ApJL, 798, L36
Coulter, D. A., Kilpatrick, C. D., Siebert, M. R., et al. 2017, Sci, https://doi.org/10.1126/science.aap9811
Dessart, L., Ott, C. D., Burrows, A., Rosswog, S., & Livne, E. 2009, ApJ, 690, 1681
Fernández, R., & Metzger, B. D. 2013, ApJ, 763, 108
Gall, C., Hjorth, J., & Andersen, A. C. 2011, A&ARv, 19, 43
Giacomazzo, B., Perna, R., Rezzolla, L., Troja, E., & Lazzati, D. 2013, ApJL, 762, L18
Goldstein, A., Veres, P., Burns, E., et al. 2017, ApJL, https://doi.org/10.3847/2041-8213/aa8f41
Gompertz, B. P., Levan, A. J., Tanvir, N. R., et al. 2017, arXiv:1710.05442
Grossman, D., Korobkin, O., Rosswog, S., & Piran, T. 2014, MNRAS, 439, 757
Hildebrand, R.-H. 1993, QJRAS, 24, 267
Hjorth, J., Levan, A. J., Tanvir, N. R., et al. 2017, ApJL, https://doi.org/10.3847/2041-8213/aa9110
Just, O., Bauswein, A., Pulpillo, R. A., Goriely, S., & Janka, H.-T. 2015, MNRAS, 448, 541
Lau, R. M., Ofek, E. O., & Kasliwal, M. M. 2017, GCN Circular, 21982
Levan, A. J., Lyman, J. D., Tanvir, N. R., et al. 2017, ApJL, https://doi.org/10.3847/2041-8213/aa905f
Li, A., & Draine, B. T. 2001, ApJ, 554, 778
Martin, D., Perego, A., Arcones, A., et al. 2015, ApJ, 813, 2
Metzger, B. D., & Fernández, R. 2014, MNRAS, 441, 3444
Metzger, B. D., Martínez-Pinedo, G., Darbha, S., et al. 2010, MNRAS, 406, 2650
Perego, A., Rosswog, S., Cabezón, R. M., et al. 2014, MNRAS, 443, 3134

Pian, E., D'Avanzo, P., Benetti, S., et al. 2017, Natur, https://doi.org/10.1038/nature24298
Rosswog, S., Feindt, U., Korobkin, O., et al. 2017, CQGra, 34, 104001
Rouleau, F., & Martin, P. G. 1991, ApJ, 377, 526
Savchenko, V., Ferrigno, C., Kuulkers, E., et al. 2017, ApJL, https://doi.org/10.3847/2041-8213/aa8f94
Siegel, D. M., & Metzger, B. D. 2017, arXiv:1705.05473
Takami, H., Nozawa, T., & Ioka, K. 2014, ApJL, 789, L6
Tanvir, N. R., Levan, A. J., Fruchter, A. S., et al. 2013, Natur, 500, 547
Tanvir, N. R., Levan, A. J., González-Fernández, C., et al. 2017, ApJL, https://doi.org/10.3847/2041-8213/aa90b6
Winteler, C. 2012, PhD thesis, Univ. Basel Switzerland
Zubko, V. G., Mennella, V., Colangeli, L., & Bussoletti, E. 1996, MNRAS, 282, 1 321